Precursor Conversion Kinetics and the Nucleation of Cadmium Selenide Nanocrystals

Jonathan S. Owen,[†] Emory M. Chan,[‡] Haitao Liu,[§] and A. Paul Alivisatos*,[⊥]

Department of Chemistry, University of California, Berkeley, and Materials Science Division, Lawrence Berkeley National Laboratory, Berkeley, California 94720, United States

Received July 29, 2010; E-mail: alivis@berkeley.edu

Abstract: The kinetics of cadmium selenide (CdSe) nanocrystal formation was studied using UV−visible absorption spectroscopy integrated with an automated, high-throughput synthesis platform. Reaction of anhydrous cadmium octadecylphosphonate (Cd-ODPA) with alkylphosphine selenides (**1**, tri-*n*-octylphosphine selenide; **2**, di-*n*-butylphenylphosphine selenide; **3**, *n*-butyldiphenylphosphine selenide) in recrystallized tri-*n*-octylphosphine oxide was monitored by following the absorbance of CdSe at $\lambda = 350$ nm, where the extinction coefficient is independent of size, and the disappearance of the selenium precursor using $\{^1H\}^{31}P$ NMR spectroscopy. Our results indicate that precursor conversion limits the rate of nanocrystal nucleation and growth. The initial precursor conversion rate (Q_o) depends linearly on [**1**] (Q_o(**1**) = 3.0−36 μM/s) and decreases as the number of aryl groups bound to phosphorus increases (**1** > **2** > **3**). Changes to Q_o influence the final number of nanocrystals and thus control particle size. Using similar methods, we show that changing [ODPA] has a negligible influence on precursor reactivity while increasing the growth rate of nuclei, thereby decreasing the final number of nanocrystals. These results are interpreted in light of a mechanism where the precursors react in an irreversible step that supplies the reaction medium with a solute form of the semiconductor.

Introduction

Reliable access to colloidal semiconductor nanocrystals (NCs) has led to numerous fundamental discoveries and technological advances.[1−12] Many years of synthetic developments[1,13,14] have provided powerful tools to prepare anisotropic shapes, branched NCs, and NC heterostructures.[15−18] Despite ready access to a variety of colloidal nanostructures, these crystallizations remain difficult to control because the mechanisms of their growth are not well understood.

Early mechanistic investigations of CdE (E = S, Se, Te) NC crystallization focused on the interaction of surfactants with crystal surfaces during nucleation and growth. A number of these studies found a link between the selective surface adhesion of alkylphosphonic acids and anisotropic crystal growth and branching.[19,20] Carboxylic, phosphonic, and phosphinic acid surfactants are also known to impact crystal nucleation and can be used to control average NC radius. For example, carboxylic acid surfactants can inhibit the nucleation of II−VI NCs, leading to an increase in the final particle size with increasing oleic acid concentration.[21−24] Among several suggestions, binding

† Current address: Department of Chemistry, Columbia University.
‡ Current address: Molecular Foundry, Lawrence Berkeley National Laboratory.
§ Current address: Department of Chemistry, University of Pittsburgh.
⊥ Current address: Lawrence Berkeley National Laboratory.

(1) Murray, C. B.; Norris, D. J.; Bawendi, M. G. *J. Am. Chem. Soc.* **1993**, *115*, 8706–8715.
(2) Talapin, D. V.; Lee, J. S.; Kovalenko, M. V.; Shevchenko, E. V. *Chem. Rev.* **2010**, *110*, 389–458.
(3) Somers, R. C.; Bawendi, M. G.; Nocera, D. G. *Chem. Soc. Rev.* **2007**, *36*, 579–591.
(4) Vanmaekelbergh, D.; Liljeroth, P. *Chem. Soc. Rev.* **2005**, *34*, 299–312.
(5) Hu, J. T.; Li, L. S.; Yang, W. D.; Manna, L.; Wang, L. W.; Alivisatos, A. P. *Science* **2001**, *292*, 2060–2063.
(6) Klimov, V. I.; Mikhailovsky, A. A.; Xu, S.; Malko, A.; Hollingsworth, J. A.; Leatherdale, C. A.; Eisler, H. J.; Bawendi, M. G. *Science* **2000**, *290*, 314–317.
(7) Collier, C. P.; Vossmeyer, T.; Heath, J. R. *Annu. Rev. Phys. Chem.* **1998**, *49*, 371–404.
(8) Chan, W. C. W.; Nie, S. M. *Science* **1998**, *281*, 2016–2018.
(9) Bruchez, M.; Moronne, M.; Gin, P.; Weiss, S.; Alivisatos, A. P. *Science* **1998**, *281*, 2013–2016.
(10) Nirmal, M.; Dabbousi, B. O.; Bawendi, M. G.; Macklin, J. J.; Trautman, J. K.; Harris, T. D.; Brus, L. E. *Nature* **1996**, *383*, 802–804.
(11) Alivisatos, A. P. *Science* **1996**, *271*, 933–937.
(12) Dabbousi, B. O.; Bawendi, M. G.; Onitsuka, O.; Rubner, M. F. *Appl. Phys. Lett.* **1995**, *66*, 1316–1318.
(13) Steigerwald, M. L.; Alivisatos, A. P.; Gibson, J. M.; Harris, T. D.; Kortan, R.; Muller, A. J.; Thayer, A. M.; Duncan, T. M.; Douglass, D. C.; Brus, L. E. *J. Am. Chem. Soc.* **1988**, *110*, 3046–3050.
(14) Peng, Z. A.; Peng, X. G. *J. Am. Chem. Soc.* **2001**, *123*, 183–184.

(15) Carbone, L.; Kudera, S.; Carlino, E.; Parak, W. J.; Giannini, C.; Cingolani, R.; Manna, L. *J. Am. Chem. Soc.* **2006**, *128*, 748–755.
(16) Li, L. S.; Hu, J. T.; Yang, W. D.; Alivisatos, A. P. *Nano Lett.* **2001**, *1*, 349–351.
(17) Peng, X. G.; Manna, L.; Yang, W. D.; Wickham, J.; Scher, E.; Kadavanich, A.; Alivisatos, A. P. *Nature* **2000**, *404*, 59–61.
(18) Manna, L.; Scher, E. C.; Alivisatos, A. P. *J. Am. Chem. Soc.* **2000**, *122*, 12700–12706.
(19) Yin, Y.; Alivisatos, A. P. *Nature* **2005**, *437*, 664–670.
(20) Peng, X. G.; Wickham, J.; Alivisatos, A. P. *J. Am. Chem. Soc.* **1998**, *120*, 5343–5344.
(21) Yordanov, G. G.; Yoshimura, H.; Dushkin, C. D. *Colloids Surf. A* **2008**, *322*, 177–182.
(22) Yu, W. W.; Peng, X. G. *Angew. Chem., Int. Ed.* **2002**, *41*, 2368–2371.
(23) Bullen, C. R.; Mulvaney, P. *Nano Lett.* **2004**, *4*, 2303–2307.
(24) van Embden, J.; Mulvaney, P. *Langmuir* **2005**, *21*, 10226–10233.

Scheme 1. Lewis Acid Activation and Phosphine Selenide Cleavage[a]
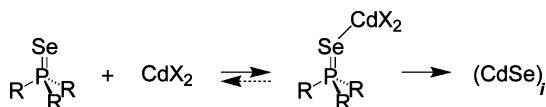
[a] CdX$_2$ refers to alkylcarboxylate and alkylphosphonate complexes of cadmium, e.g., Cd-ODPA in this study. (CdSe)$_i$ refers to a solute form of CdSe.

between oleic acid and the starting cadmium ion or the surfaces of nuclei was proposed as the origin of its inhibitory effect.

Less is known about the kinetics of reaction between precursor molecules and its influence on NC formation.[25−27] Only recently have detailed studies of the microscopic steps that control the precursor reaction begun to appear. For example, cadmium−alkylphosphonate and −alkylcarboxylate complexes have been shown to bind tri-*n*-alkylphosphine chalcogenides, activating them toward nucleophilic attack and P=E bond cleavage (Scheme 1).[28] Related Lewis-acid activation mechanisms have also been shown for II−IV[29] and III−V[30] NCs, while other syntheses appear to follow multistep pathways via heterogeneous intermediates.[31,32] The relationship between these reaction pathways and crystallization is unclear for semiconductor NCs, although it has been a subject of study in transition metal NCs.[33]

In many colloidal crystallizations,[34] the precursor reaction is an integral part of monodisperse particle formation since it provides an internal reservoir of solute that is continually released during the crystallization. Under the right conditions, a balance between solute production and consumption during growth can maintain the supersaturation at a level that causes size distribution focusing.[35] In these cases, precursor reaction kinetics can play an important role in the resultant crystal size and size distribution. While the kinetics of solute supply is a well-developed avenue of study in canonical colloidal crystallizations, it is a relatively unstudied aspect of NC syntheses.

High-temperature colloidal crystallizations have been studied using flow cells,[36] microfluidic chips,[37,38] *in situ* absorption spectroscopy,[39] and timed aliquoting of the reaction mixture.[21−25]

However, NCs display temperature-dependent optical properties, making it a challenge to monitor CdSe NCs growing *in situ*. As a result, most researchers have undertaken such studies by timed aliquoting of the reaction mixture and room-temperature analysis of the NC optical properties. Obtaining precise kinetics data with these methods is challenging, given the air sensitivity of the reaction mixture, the high temperatures of these crystallizations, and the labor-intensive nature of quantitative aliquoting. In order to address these challenges, we have employed an automated, high-throughput reactor to measure reaction kinetics, which was previously reported by Chan et al. to greatly aid in synthetic reproducibility.[31] This instrument provides precise control over the reaction temperature as well as the timing of the injection and aliquots and allows precise dilution of aliquots to a known concentration for quantitative absorption spectroscopy, all within an inert atmosphere glovebox.

In the present study we explore the relationship between the precursor reaction mechanism, the kinetics of precursor conversion, and the final number of NCs. Our observations indicate that phosphine selenides and anhydrous cadmium octadecylphosphonate undergo a slow chemical reaction that continuously liberates CdSe to the reaction medium, causing supersaturation, nucleation, and NC growth. The reliability of our study is ensured by the well-defined composition of our reagents, the purity of which has an important influence on colloidal crystallizations.[40−42] Our results highlight the importance of the precursor conversion to crystal nucleation and suggest that reproducible NC syntheses can be designed using well-defined starting materials and carefully tuned reactivity.

Results

Reaction of Phosphine Selenides with Cadmium Octadecylphosphonate. Cadmium selenide NCs were prepared using carefully purified reagents shown to eliminate inconsistencies across different sources of starting material.[40,41,43] Anhydrous cadmium octadecylphosphonate (Cd-ODPA) was prepared by dropwise addition of a 2:1 tri-*n*-octylphosphine:CdMe$_2$ solution to molten tri-*n*-octylphosphine oxide (TOPO) and octadecylphosphonic acid (ODPA, 1.67−2.0 equiv) at 275 °C.[44] At low ODPA:Cd ratios, the Cd-ODPA coordination polymer becomes insoluble at this temperature and dissolves only upon heating.[45,46] At 1.67 equiv of ODPA and above, the reaction mixture is clear and colorless at 325 °C, while at lower ODPA: Cd ratios, the precipitate does not completely dissolve, resulting in irregularly branched NCs. All reactions were run with at least

(25) Yordanov, G. G.; Dushkin, C. D.; Adachi, E. *Colloids Surf. A* **2008**, *316*, 37–45.
(26) Viswanatha, R.; Amenitsch, H.; Sarma, D. D. *J. Am. Chem. Soc.* **2007**, *129*, 4470–4475.
(27) Chen, O.; Chen, X.; Yang, Y. A.; Lynch, J.; Wu, H. M.; Zhuang, J. Q.; Cao, Y. C. *Angew. Chem., Int. Ed.* **2008**, *47*, 8638–8641.
(28) Liu, H. T.; Owen, J. S.; Alivisatos, A. P. *J. Am. Chem. Soc.* **2007**, *129*, 305–312.
(29) Steckel, J. S.; Yen, B. K. H.; Oertel, D. C.; Bawendi, M. G. *J. Am. Chem. Soc.* **2006**, *128*, 13032–13033.
(30) Allen, P. M.; Walker, B. J.; Bawendi, M. G. *Angew. Chem., Int. Ed.* **2010**, *49*, 760–762.
(31) Chan, E. M.; Xu, C.; Mao, A. W.; Han, G.; Owen, J. S.; Cohen, B. E.; Milliron, D. J. *Nano Lett.* **2010**, *10*, 1874–1885.
(32) Joo, J.; Pietryga, J. M.; McGuire, J. A.; Jeon, S. H.; Williams, D. J.; Wang, H. L.; Klimov, V. I. *J. Am. Chem. Soc.* **2009**, *131*, 10620–10628.
(33) Finney, E. E.; Finke, R. G. *J. Colloid Interface Sci.* **2008**, *317*, 351–374.
(34) Sugimoto, T. *Monodispersed Particles*; Elsevier: Amsterdam, 2001; see especially Chapter 7.
(35) Sugimoto, T. *Adv. Colloid Interface* **1987**, *28*, 65–108.
(36) Yen, B. K. H.; Stott, N. E.; Jensen, K. F.; Bawendi, M. G. *Adv. Mater.* **2003**, *15*, 1858–1862.
(37) Yen, B. K. H.; Gunther, A.; Schmidt, M. A.; Jensen, K. F.; Bawendi, M. G. *Angew. Chem., Int. Ed.* **2005**, *44*, 5447–5451.
(38) Chan, E. M.; Mathies, R. A.; Alivisatos, A. P. *Nano Lett.* **2003**, *3*, 199–201.
(39) Qu, L. H.; Yu, W. W.; Peng, X. P. *Nano Lett.* **2004**, *4*, 465–469.

(40) Wang, F. D.; Tang, R.; Buhro, W. E. *Nano Lett.* **2008**, *8*, 3521–3524.
(41) Wang, F.; Tang, R.; Kao, J. L. F.; Dingman, S. D.; Buhro, W. E. *J. Am. Chem. Soc.* **2009**, *131*, 4983–4994.
(42) Kopping, J. T.; Patten, T. E. *J. Am. Chem. Soc.* **2008**, *130*, 5689–5698.
(43) Owen, J. S.; Park, J.; Trudeau, P. E.; Alivisatos, A. P. *J. Am. Chem. Soc.* **2008**, *130*, 12279–12281.
(44) Cd-ODPA refers to the mixture of octadecylphosphonic acid and cadmium octadecylphosphonate that results from the protonolysis of dimethylcadmium with octadecylphosphonic acid. Our observations suggest this starting material is a coordination polymer, even at the growth temperature (vide infra). Thus, Cd-ODPA generally refers to a polymeric species of cadmium ions bridged by octadecylphosphonic acid and octadecylphosphonate moieties.
(45) Cao, G.; Lynch, V. M.; Yacullo, L. N. *Chem. Mater.* **1993**, *5*, 1000–1006.
(46) Methane is evolved during this addition, and at the same time the surface tension of the solution increases due to the polymer formation. At low ODPA:Cd ratios, a foam often forms at the surface of the reaction mixture that can cause the last few drops of CdMe$_2$ to decompose thermally rather than by reaction with the phosphonic acid.
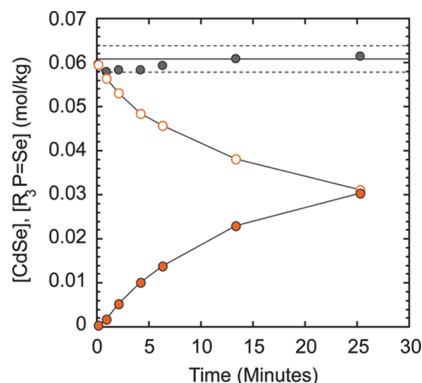
Figure 1. Comparison of the phosphine selenide conversion (empty circles, **1**) and appearance of CdSe (solid orange circles) versus time as measured by $\{^1H\}^{31}P$ NMR spectroscopy and nanocrystal absorbance at 350 nm. The sum of these measures (solid gray circles) matches the theoretical total (—) within the ~10% uncertainty of our NMR measurements (---). For error analysis, see Supporting Information.

1.67 equiv of ODPA to obtain quasi-spherical colloids (Figure S1, Supporting Information).

Upon thermal equilibration at 325 °C, phosphine selenides **1–3** are injected into the TOPO solution of Cd-ODPA to initiate the reaction (**1**, tri-*n*-octylphosphine selenide; **2**, di-*n*-butylphenylphosphine selenide; **3**, *n*-butyldiphenylphosphine selenide). After an induction period ($t_{induction} = 1–5$ min) where the reaction mixture is clear and colorless, a yellow color slowly develops that evolves to red and then brown over the course of 5–15 min, signaling the growth of CdSe. NCs with narrow size distributions (diameter = 2–6 nm; PL fwhm = 30 ± 4 nm) are consistently formed under our optimized conditions (Figures S1 and S2, Supporting Information).[47]

Monitoring Precursor Reaction Kinetics. Disappearance of the phosphine selenide (**1–3**) and appearance of its corresponding phosphine oxide were monitored with $\{^1H\}^{31}P$ NMR spectroscopy. These data were compared with the molar concentration of crystalline CdSe we extracted from the size-independent NC absorbance at $\lambda = 350$ nm (Figure 1). The correlation between these measurements accounts for >95 ± 5% of the added selenium in the form of phosphine selenide or NCs (Figure 1).[48,49] Phosphine selenide conversion is plotted against the yield of CdSe in Figure 2 for a series of phosphine selenides with aryl and alkyl substituents bound to phosphorus (**1–3**). In these reactions, the precursor conversion approaches ~50% after 20 min for **1**, while the slowest reaction (**3**) reaches only ~20% conversion in the same time frame. From this plot it is clear that replacing aliphatic chains with aryl substituents slows the rate of phosphine selenide conversion.

With our automated synthesis platform we investigated how changes in [**1**], [Cd-ODPA], and [ODPA] influenced the appearance of CdSe versus time (Figures 3 and 4 and Table S1, Supporting Information). In order to make quantitative comparisons between reactions, the initial precursor reaction rate (Q_o) was estimated from plots of [CdSe] versus time (see Experimental Section). These data were analyzed as a function of the precursor concentrations, showing that Q_o is linearly

(47) At high conversion of Cd-ODPA, e.g., long reaction times, or at low [Cd-ODPA], a second nucleation event is sometimes observed (see Supporting Information).
(48) Yu, W. W.; Qu, L. H.; Guo, W. Z.; Peng, X. G. *Chem. Mater.* **2003**, *15*, 2854–2860.
(49) Leatherdale, C. A.; Woo, W. K.; Mikulec, F. V.; Bawendi, M. G. *J. Phys. Chem. B* **2002**, *106*, 7619–7622.
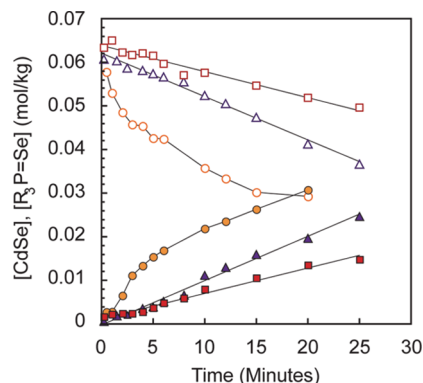
Figure 2. Comparison of the phosphine selenide conversion (empty symbols) and appearance of CdSe (filled symbols) versus time in reactions with **1–3** (**1**, orange circles; **2**, purple triangles; **3**, red squares) as measured by $\{^1H\}^{31}P$ NMR spectroscopy and the nanocrystal absorbance at 350 nm. For error analysis, see Supporting Information.
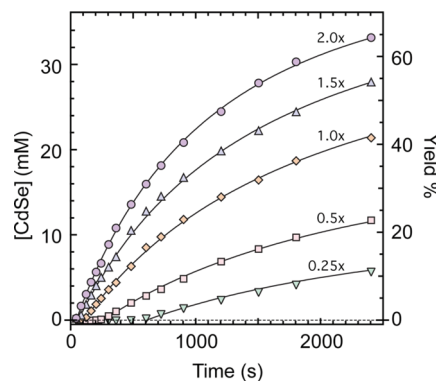

Figure 3. Appearance of CdSe versus time at several concentrations of added phosphine selenide (0.25–2.0 equiv). An induction period is visible at early times where there is zero absorbance at 350 nm (---). Solid lines are included as a guide to the eye. For error analysis, see Supporting Information.
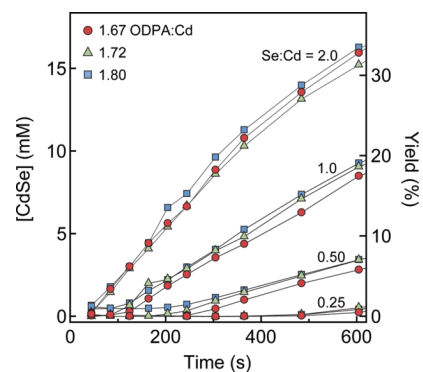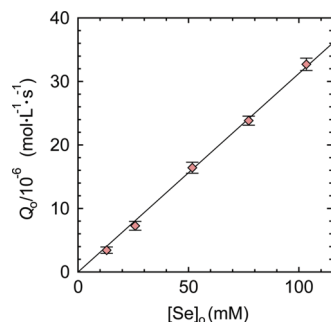

Figure 4. Appearance of CdSe at early times for several concentrations of added phosphine selenide (0.25, 0.5, 1.0, 2.0 equiv) and three concentrations of ODPA (1.67, 1.72, 1.80 equiv). For error analysis, see Supporting Information.

dependent on [Cd-ODPA] and [**1**] (Figures 5 and 6). On the other hand, increasing [ODPA], albeit over a small range, had a negligible effect on Q_o, despite a substantial effect on the particle size (Figure 4).

In fast reactions, the initial rate of phosphine selenide conversion matched well with the initial rate of CdSe appearance. However, in slow reactions, our estimate of Q_o is significantly influenced by the induction period that precedes the appearance of the NC absorption. This induction is clearly

Figure 5. Initial reaction rate (Q_o) versus concentration of added Se ([Se]$_o$) (0.25–2.0 equiv) obtained by measuring the slope at early time in Figure 3 ([Cd-ODPA]$_o$ = 52 mM). For error analysis, see Supporting Information.
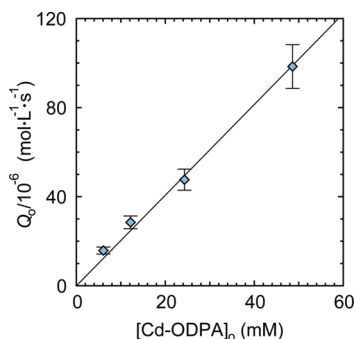

Figure 6. Initial reaction rate (Q_o) versus initial concentration of Cd-ODPA ([Se]$_o$ = 192.7 mM). For error analysis, see Supporting Information.
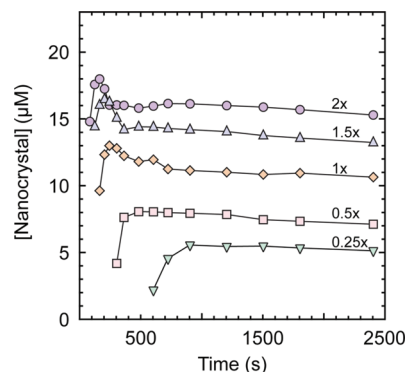

Figure 7. Temporal evolution of [nanocrystal] across several concentrations of added phosphine selenide (**1**) (0.25–2.0 equiv). For error analysis, see Supporting Information.
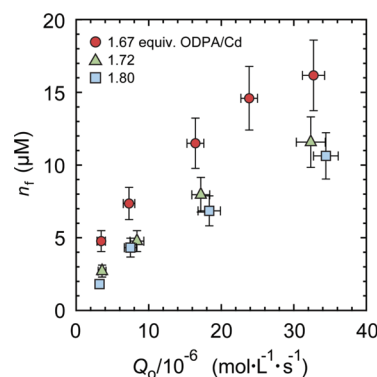

Figure 8. n_f versus Q_o obtained from several concentrations of ODPA (red circle, 1.67 equiv; green triangle, 1.72 equiv; blue square, 1.80 equiv) and tri-*n*-octylphosphine selenide ([**1**] = 13–154 mM; Q_o = 3–37 μM/s). Error in n_f reflects an uncertainty of 0.2 nm in the average radius (see discussion in the Supporting Information).

visible in Figures 2 and 3, where NC absorbance does not appear for as long as 10 min in the slowest case. Despite this lag in the absorbance at 350 nm, there is a measurable conversion of the phosphine selenide (<∼5%). Initial rates in these cases could be estimated from the increase in absorption after the lag period or by fitting a line through the intercept that includes the first few points after the lag (see Experimental Section). These methods produce similar estimates of Q_o, with ∼15% relative deviation from the mean in the slowest reactions and only ∼5% in the fastest reactions.

Nanocrystal Concentration. In experiments with preformed Cd-ODPA, particles evolve in size from approximately 3 to 7 nm as ∼0.10–0.50 mmol of CdSe is formed. This corresponds to 3–14 μM solutions of NCs, assuming they have a spherical shape and a molar volume equal to that of the bulk material. The temporal evolution of the [NC] is plotted in Figure 7. After the first few minutes of reaction, the [NC] stabilizes and remains nearly constant over the course of the reaction. An average of the [NC] at each time point after the initial fluctuation was used to calculate the NC concentration after nucleation (n_f). This measure of particle number was analyzed as a function of the reagent concentration and structure of the phosphine selenide. Greater n_f resulted from reactions run with higher concentration of [**1**] and [Cd-ODPA] and was sensitive to the structure of the phosphine selenide (n_f(**3**) < n_f(**2**) < n_f(**1**)). The range in n_f obtained by these changes corresponds to a ∼2.1× range in diameter at an equivalent % conversion (Table S1).

We analyzed the relationship between the precursor reaction rate and the number of NCs in Figure 8 and Figure S5 (Supporting Information). Increasing the initial rate led to a greater number of NCs, both when changing the structure of the phosphine selenide (**1–3**) and when increasing [**1**] and Cd-ODPA. However, increasing [ODPA] had a small impact on
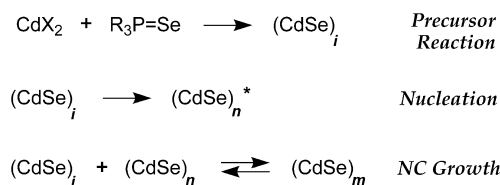
the precursor reaction rate and, at the same time, had an obvious inverse effect on the number of NCs (Figure 8).

Reaction by Rapid, Simultaneous Injection of CdMe$_2$ and Tri-*n*-octylphosphine Selenide. CdSe NCs were also prepared by rapidly injecting a mixture of CdMe$_2$ and **1** into molten TOPO and ODPA, in analogy to the synthetic method reported by Bawendi.[1] Upon injection, gas vigorously evolved from the solution and the color rapidly changed, signaling the growth of CdSe. Aliquots taken immediately following the injection show that **1** is rapidly consumed ($t < 40$ s), which is matched by an equally rapid appearance of CdSe (Figure S6, Supporting Information). After this initial burst, precursor conversion continues at a rate similar to that of reactions run with preformed Cd-ODPA. Rapid injection of this precursor solution into pure TOPO without added ODPA results in rapid formation of a turbid, dark brown mixture ($t < 5$ s). Analysis of the dark solid isolated from this mixture with X-ray diffraction confirmed the formation of CdSe as well as cadmium metal. In addition, increased [ODPA] substantially inhibits this burst of CdSe formation.[50]

Discussion

The experiments presented above support a mechanism where precursors act as a reservoir that slowly releases a solute[51] form

(50) Although the extant of this burst of reaction is sensitive to the conditions of injection, in one study adding an additional 0.5 equiv of ODPA reduced this initially rapid conversion from 30% to 10%.

**Scheme 2.** Precursor Conversion to Solute and Its Subsequent Crystallization[a]

$$CdX_2 + R_3P{=}Se \longrightarrow (CdSe)_i \qquad \textit{Precursor Reaction}$$

$$(CdSe)_i \longrightarrow (CdSe)_n^* \qquad \textit{Nucleation}$$

$$(CdSe)_i + (CdSe)_n \rightleftharpoons (CdSe)_m \qquad \textit{NC Growth}$$

[a] $(CdSe)_i$ refers to a solute form of CdSe, $(CdSe)_n$ refers to nanocrystals, and $(CdSe)_n^*$ refers to nuclei.

of CdSe over the course of the crystallization (Scheme 2). Accumulation of the solute leads to supersaturation until a "critical" concentration is reached and nucleation begins. Thus, under our conditions, the slow reaction between precursors limits the rate of NC nucleation and growth. This conclusion is clear from the similarity between the phosphine selenide conversion and CdSe yield, the dependence of the CdSe formation kinetics on precursor concentration, and its relationship to the final number of NCs (n_f). In addition, the reaction rate is sensitive to the concentration of precursors and phosphine selenide structure in a fashion that is consistent with our previously proposed Lewis-acid activation pathway. These characteristics support a La Mer-like nucleation and growth mechanism that is distinctly different from other syntheses, where Ostwald ripening or surface autocatalysis appear to dominate the kinetics of particle growth.[33,52−54]

Kinetics and Mechanism of the Precursor Conversion. Comparison of ^{31}P NMR and UV−visible absorption spectroscopy measurements showed a 1:1 correlation between the moles of **1−3** consumed and moles of CdSe in the form of NCs. Only during the induction period was a small percentage of the phosphine selenide converted to its phosphine oxide (<5%) without an increase in the NC absorption. Presumably, during the induction, the converted precursor increases the concentration of solute until nucleation takes place and NCs appear in the absorption spectrum.[55] By calculating the conversion at the end of the induction period using the initial reaction rate, we obtain a rough estimate of the solute concentration preceding nucleation (1.6 ± 1.0 mM, 3% conversion).[56]

This interpretation suggests that aliquots taken at the end of the induction period contain solute concentrations close to or beyond the solubility limit, and yet they show little absorbance at 350 nm. Thus, our measure of [CdSe] taken from the absorption at 350 nm gives a direct measure of the molar

Scheme 3. Binding and Cleavage Reaction Mechanism

1: $R_1 = R_2 = R_3$ = Octyl
2: $R_1 = R_2$ = Butyl, R_3 = Ph
3: R_1 = Butyl, $R_2 = R_3$ = Ph
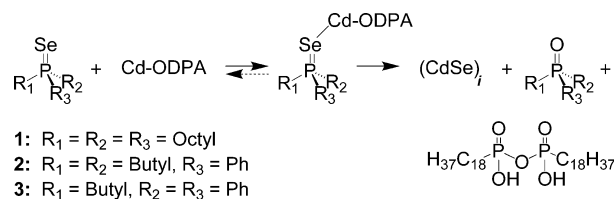
concentration of CdSe in the form of NCs and is not complicated by absorption from solute. The conversion is, therefore, approximately equal to the yield of crystalline CdSe, allowing us to estimate precursor reaction kinetics indirectly from the absorbance of NCs. Furthermore, this correlation between precursor conversion and CdSe yield holds across an order of magnitude in reaction rates, suggesting that the evolution of [CdSe] is controlled by the precursor reaction rate rather than by the kinetics of solute crystallization.

The precursor conversion rate is sensitive to differences in the structure of the phosphine selenide (**1−3**). As aliphatic chains are replaced with aryl substituents, the reaction slows and the yield is reduced ($Q_o(\mathbf{3}) < Q_o(\mathbf{2}) < Q_o(\mathbf{1})$, Figure 2). Aryl substituents are known to inhibit the binding of the parent phosphines to Ni(0) and should have a similar effect on the binding constants of **1−3** to cadmium.[57] They may also inhibit attack of the phosphonate nucleophile. These trends are both consistent with our previously proposed Lewis-acid activation mechanism (Scheme 3).

Using our high-throughput synthesis platform, we investigated the concentration dependence of Q_o and found it to depend linearly on both [**1**] and [Cd-ODPA].[58,59] Similarly, these changes are consistent with the mechanism proposed in Scheme 3, and can be explained by the rate-determining binding of phosphine selenide to the cadmium center or by a rapid preequilibrium between free and bound **1** preceding rate-determining P=E bond cleavage. Our observations do not conclusively demonstrate whether binding or cleavage is the rate-determining step, since we did not observe saturation in the rate as a function of **1** or Cd-ODPA.

While **1** is known to form stable complexes with cadmium carboxylates prior to its cleavage,[28] we did not find evidence for a stable complex between **1** and Cd-ODPA in the ^{31}P NMR spectra of reaction aliquots in this study or in a previous one.[28] If binding is a rapid preequilibrium step, the net precursor conversion rate will also be determined by the cleavage step. However, the precise nature of the nucleophilic attack is obscured by the polymeric structure of the Cd-ODPA used in this study.[45] As a result, nucleophilic attack may involve either a unimolecular rearrangement of the TOPSe−Cd-ODPA complex or attack by a neighboring ODPA fragment and result in a cleavage step that is insensitive to changes in [ODPA] or [Cd-ODPA]. On the other hand, water is known to accelerate the precursor conversion, perhaps by serving as a more reactive

(51) The term "solute" refers to a solution species produced by the precursor reaction that has not undergone nucleation or addition to a nanocrystal. Using the perhaps more familiar term "monomer" in this discussion is misleading since it implies something about the structure of this solution species. For example, the solute may be composed of multiple monomer units and may depending on the monomer concentration, temperature, and composition of the reaction medium.

(52) Tiemann, M.; Marlow, F.; Brieler, F.; Linden, M. *J. Phys. Chem. B* **2006**, *110*, 23142−23147.

(53) Brazeau, A. L.; Jones, N. D. *J. Phys. Chem. C* **2009**, *113*, 20246−20251.

(54) Viswanatha, R.; Amenitsch, H.; Santra, S.; Sapra, S.; Datar, S. S.; Zhou, Y.; Nayak, S. K.; Kumar, S. K.; Sarma, D. D. *J. Phys. Chem. Lett.* **2010**, *1*, 304−308.

(55) The smallest nanocrystals visible after the the induction period have an absorption wavelength of their $1S_{1/2e}−1S_{3/2h}$ transition at ∼490 nm.

(56) In principle, other forms of CdSe, for example solute, could contribute to the absorption at 350 nm. However, the dissolution experiments discussed below indicate that the equilibrium solubility of CdSe in the reaction medium is low under our conditions and is unlikely to contribute to the total absorption to an extent that obscures our results.

(57) Hartwig, J. R. *Organotransition Metal Chemistry: From Bonding to Catalysis*; University Science Books: Sausalito, CA, 2010; pp 9.

(58) Espenson, J. H. *Chemical kinetics and reaction mechanisms*; McGraw-Hill: New York, 1981.

(59) This is somewhat surprising, given that many time traces for precursor cleavage do not show an exponential decay and instead show a roughly linear decay. We suggest this behavior may result from an increasing Lewis acidity of the Cd-ODPA coordination polymer upon conversion of the phosphonate ligands to their anhydride form. This increasing Lewis acidity may result in more favorable phosphine selenide binding and cleavage at longer reaction times.

nucleophile than ODPA.[28] Given that binding to cadmium carboxylate complexes is rapid and reversible and the rate acceleration is caused by water, we favor a mechanism where binding of **1** by Cd-ODPA is likely to be a rapid preequilbrium step that precedes P=Se cleavage.

Nucleation and Precursor Reaction Rate. We have obtained evidence for a correlation between the final number of NCs (n_f) and the initial rate of the precursor conversion (Q_o) (Figures 8 and S5). This behavior is evident from experiments where increasing [**1**] led to a faster reaction rate and a smaller average particle radius. Similarly, the conversion rate and n_f were decreased 8-fold by changing the structure of the phosphine selenide and without changing the concentration (Figure S4). This relationship suggests a link between the rate of solute supply during nucleation and the number of nucleation events.

Sugimoto and co-workers have documented a similar relationship in their studies of colloidal silver halide crystallization.[60,61] These observations can be explained by a theory of nucleation that is summarized by eq 1 below. In this model, the production of solute during the nucleation stage ($Q_o V_m$, cm^{3}L^{-1}s^{-1}; V_m is the molar volume) leads to either the formation of critical nuclei (v^*(dn/dt); v^* is the volume of the critical nucleus) or their growth (vn_t; v is the nucleus growth rate and n_t is the number of nuclei). Assuming that the nucleation rate is "critically" dependent on [solute] above the nucleation threshold, any increase in solute production is compensated by the formation of nuclei. Thus, the solute concentration, and therefore, the growth rate of nuclei (v), is effectively constant during this period. By integrating eq 1 over the length of the nucleation stage ($t = 0 \rightarrow \infty$), one can obtain eq 2, where the number of stable crystals is proportional to the rate of solute supply (Q_o) and inversely proportional to the volumetric growth rate of the nucleus (v).[60]

$$Q_o V_m = v^* \frac{dn}{dt} + vn_t \tag{1}$$

$$n_f = \frac{Q_o V_m}{v} \tag{2}$$

While we do observe an increase in n_f as the initial precursor reaction rate increases, the dependence of n_f on Q_o measured in this study does not appear to be linear. It is unclear whether this deviation reflects a real kinetic difference between the present study and previous ones, or if it is an artifact of our analysis. Among possible explanations, the change in [TOPSe] that accompanies the increasing Q_o in Figure 8 may also influence the nucleus growth rate (a similar effect of changing [ODPA] is discussed below). The curvature may also be explained by a nucleation rate that is less than "critically" dependent on solute concentration. Instead, the nucleus growth rate may be relatively sensitive to small changes in solute concentration during the nucleation phase, and the curvature may reflect an increase in the rate of nucleus growth as Q_o is increased.

A number of experimental uncertainties obscure this result, however, particularly systematic error in our estimate of the NCs average molar volume, which we use to calculate n_f. This is particularly noticeable at small sizes, where uncertainty in

the average radius as well as radius-dependent NC stoichiometry make it difficult to measure n_f.[62-64] For example, assuming the TEM measurements used by Yu et al. have a precision equal to a CdSe bond distance ($\sim\pm0.2$ nm), uncertainty in the volume of the smallest NCs ($d \approx 2.3$ nm) is at least 30%. This inherent error in volume and a lack of data on the radius-dependent NC stoichiometry suggest that fluctuations in the particle concentration versus time should be interpreted with caution, particularly at early times when the NCs are smallest. More accurate determination of [NC] is necessary before changes in n_f can be interpreted in detail.[65,66]

Our plot of n_f versus Q_o also reflects the well-documented increase in particle size as the surfactant (ODPA) concentration is increased (Figure 8). This observation has been suggested to originate from the strong binding between surfactants and the NC surface, which slows their growth, or between surfactants and the Cd precursor, thereby decreasing its reactivity. However, the range of [ODPA] used in this study has a negligible effect on the precursor conversion rate and a substantial impact on the particle size. Furthermore, based on the nucleation model proposed by Sugimoto, increasing [ODPA] must also *increase* the rate at which nuclei grow to a stable size during the nucleation phase (v), thereby decreasing the final number of NCs (eq 2). Preliminary studies in our laboratory show that ODPA catalyzes Ostwald ripening, which may provide a mechanism by which nuclei grow more rapidly as [ODPA] is increased (see Supporting Information). A similar conclusion was reached by Dushkin and co-workers in their studies of CdSe growth in the presence of stearic acid[21] and may also explain the relationship between average NC size and carboxylic, phosphonic, and phosphinic acid concentration described by Mulvaney and Peng.[22-24]

Simultaneous Injection of CdMe$_2$ and 1. We modeled the reaction first reported by Bawendi and co-workers by rapidly injecting a mixture of CdMe$_2$ and **1** into TOPO and ODPA.[67] These reactions showed much more rapid initial rates and resulted in nearly immediate CdSe formation, unlike when **1** is reacted with premade Cd-ODPA. This rapid burst of reactivity is competitive with the kinetics of mixing and led to reaction rates that were sensitive to conditions of the injection as well the stirring rate. In addition, increasing [ODPA] inhibited the extent of the burst. These factors suggest that this initially rapid reaction is caused by a partial thermal decomposition of CdMe$_2$, which on its own will rapidly decompose to cadmium metal at the reaction temperature or to a mixture of Cd metal and insoluble CdSe in the presence of **1**.[68] Thermolysis of CdMe$_2$ could thereby produce a burst of solute, perhaps via formation

(60) Sugimoto, T.; Shiba, F.; Sekiguchi, T.; Itoh, H. *Colloids Surf. A* **2000**, *164*, 183–203.

(61) Sugimoto, T.; Shiba, F. *Colloids Surf. A–Physicochem. Eng. Aspects* **2000**, *164*, 205–215.

(62) Moreels, I.; Lambert, K.; De Muynck, D.; Vanhaecke, F.; Poelman, D.; Martins, J. C.; Allan, G.; Hens, Z. *Chem. Mater.* **2007**, *19*, 6101–6106.

(63) Dai, Q. Q.; Wang, Y. N.; Li, X. B.; Zhang, Y.; Pellegrino, D. J.; Zhao, M. X.; Zou, B.; Seo, J.; Wang, Y. D.; Yu, W. W. *ACS Nano* **2009**, *3*, 1518–1524.

(64) Moreels, I.; Lambert, K.; Smeets, D.; De Muynck, D.; Nollet, T.; Martins, J. C.; Vanhaecke, F.; Vantomme, A.; Delerue, C.; Allan, G.; Hens, Z. *ACS Nano* **2009**, *3*, 3023–3030.

(65) Xie, R. G.; Li, Z.; Peng, X. G. *J. Am. Chem. Soc.* **2009**, *131*, 15457–15466.

(66) Nonetheless, while average radius is a major source of uncertainty at small sizes, our measure of n_f is extracted from the spectra of the largest NCs (5–7 nm), where error in radius has a much smaller impact on the calculated particle volume.

(67) A series of recent papers have highlighted the role of acidic impurities in TOPO on the crystallization and passivation of II–VI nanomaterials.

(68) Cabot, A.; Smith, R. K.; Yin, Y. D.; Zheng, H. M.; Reinhard, B. M.; Liu, H. T.; Alivisatos, A. P. *ACS Nano* **2008**, *2*, 1452–1458.

Scheme 4. Thermal and Protolytic Mechanisms of CdMe₂ Decomposition[a]
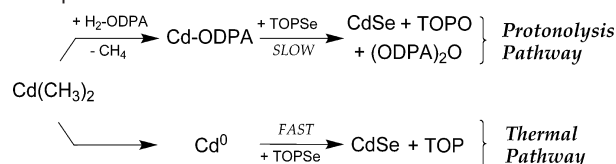
[a] (ODPA)₂O refers to the phosphonic acid anhydride formed in the P=Se cleavage reaction.

of Cd⁰ or other direct pathways.[69,70] The extent of this thermolysis is dependent on the efficiency of mixing with the TOPO solution and on the concentration of ODPA, suggesting it also undergoes competitive protonation by the phosphonic acid (Scheme 4).

Given the relationship between the initial rate of the precursor reaction and the number of NCs, reactions with an initial burst of reactivity that cannot be precisely controlled will lead to irreproducibility in synthesis. Contamination of commercial TOPO with small concentrations of acid impurities can also lead to irreproducibility in synthesis, since these impurities have a strong effect on the final particle number by changing the growth rate or by effecting the initially rapid CdMe₂ decomposition. In the present kinetics study, we were able to isolate these experimental variables by preparing anhydrous Cd-ODPA using carefully purified reagents. This allowed for slow reaction kinetics and induction times longer than the time required to achieve thorough mixing. As a result, these reactions produced a reliable rate of solute supply at well-defined concentrations of ODPA necessary for reproducible control over the number of nuclei.

Development of new syntheses and scale-up of existing reactions will benefit from a deeper understanding of the kinetic pathways by which precursors undergo reaction.[25,27–30,71,72] With this information, NC syntheses can be optimized to produce a particular size in high yield. In addition, controlled precursor reactivity can be used to maintain a relatively high supersaturation during NC growth, thereby facilitating size distribution focusing.[31,35,73] Precise tuning of precursor reactivity by the design and study of new reagents will aid this endeavor and lead to finer degrees of control in NC synthesis.

Conclusions

Our study documents nanocrystal syntheses where nucleation and particle growth are limited by the formation of solute from precursor molecules. We find strong evidence for a link between the initial precursor reaction rate and the number of NCs at the end of the reaction. In this kinetic regime, size control can be obtained by tuning the reactivity of precursor molecules. Hence, a mechanistic understanding of the precursor reaction provides insight that can be used to tune NC properties. The relationship between the structure of the phosphine selenide and its reactivity and the dependence of reaction rate on concentration are both

consistent with the pre-equilibrium Lewis-acid activation and nucleophilic attack model presented by us earlier.[28] We conclude that acid surfactants, like ODPA, may influence the average NC radius by increasing the growth rate of nuclei, thereby decreasing the number that reach a stable size, rather than by changing the reactivity of the precursor. Relatively small variations in [ODPA] proved to have a strong influence on the average NC radius, underscoring the importance of carefully removing the impurities that influence nucleation or reaction kinetics.

Experimental Section

General Methods. All air- and/or moisture-sensitive compounds were manipulated using standard Schlenk techniques or in a glovebox under an argon atmosphere. Selenium shot (99.99%) and anhydrous toluene, hexane, and chloroform were purchased from Aldrich and stored in a glovebox. Acetone was purchased from Aldrich and stored over 3 Å molecular sieves in the glovebox. *n*-Octadecylphosphonic acid (Polycarbon Industries) and tri-*n*-octylphosphine oxide (99% Reagent grade Plus, Aldrich) recrystallized as described previously.[43] Toluene-*d₈* was dried with sodium and benzophenone prior to distillation and storage under argon. Tri-*n*-octylphosphine was purchased from Strem Chemicals and stored in the glovebox. Dimethylcadmium was purchased from Strem Chemicals, vacuum transferred in the absence of light, and stored in an amber jar in the glovebox freezer. **CAUTION!** *Dimethylcadmium is extremely toxic and has high vapor pressure at room temperature. Care must be taken to thoroughly quench dimethylcadmium prior to handling contaminated glassware outside of the glovebox or fumehood.* NMR spectra were recorded on Bruker AVQ-400 and DRX-500 spectrometers.

Injection Solutions. Dimethylcadmium (1.612 g, 11.31 mmol) was weighed into a vial in the glovebox and diluted with 2 equiv of tri-*n*-octylphosphine (8.388 g, 22.63 mmol) to a total mass of 10 g. The clear, colorless solution was tightly sealed, mixed thoroughly, and stored in the glovebox freezer. Selenium shot (0.893 g, 11.31 mmol) was weighed into a vial to which was added tri-*n*-octylphosphine (9.107 g, 24.57 mmol) to a total mass of 10 g. A small stir bar was added, the vial tightly sealed, and the mixture left stirring overnight until all the solids had dissolved. This solution was stored at room temperature in the glovebox until needed. Neat **1** was prepared by stirring excess selenium shot with tri-*n*-octylphosphine overnight. The remaining selenium was removed by centrifugation. Solutions of **1** in octadecene were prepared by dilution of the neat **1** with ODE.

Synthesis of 2 and 3. Di-*n*-butylphenylphosphine and *n*-butyldiphenylphosphine were prepared by alkylation of diphenyl-chlorophosphine or phenyldichlorophosphine with *n*-butyllithium in anhydrous diethyl ether, distilled under full vacuum, and stored in a glovebox. Solutions of **2** and **3** (1.131 mmol/g) were prepared from their respective phosphines by stirring with sufficient selenium shot to obtain the desired concentration.

Reactions Conducted by Hand. a. Synthetic Protocol. Kinetics experiments shown in Figures 1 and 2 were conducted by hand in 50 mL three-neck round-bottom flasks under conditions reported earlier.[43] Briefly, dropwise addition of TOP/CdMe₂ to a mixture of ODPA and TOPO at 275 °C produced anhydrous TOPO solutions of Cd-ODPA. The reaction vessel was then heated to 325 °C, and **1** was injected to initiate the reaction. The temperature was lowered to 315 °C for the remainder of the reaction.

b. Simultaneous Injection of CdMe₂ and 1. Equal parts of the TOP/CdMe₂ and TOP/**1** solutions were mixed in the glovebox, and then the sample was wrapped in foil, removed from the glovebox, and rapidly injected into the mixture of ODPA and TOPO at 330 °C. The injection process caused vigorous bubbling of the reaction mixture and the formation of a fine white mist that escaped from the reaction vessel via an oil bubbler. After the injection, the temperature controller was lowered to 315 °C and the reaction

(69) ³¹P NMR spectra of these reaction byproducts showed the presence of TOP as well as a number of other unidentified byproducts.
(70) Steigerwald, M. L.; Sprinkle, C. R. *J. Am. Chem. Soc.* **1987**, *109*, 7200–7201.
(71) Bullen, C.; van Embden, J.; Jasieniak, J.; Cosgriff, J. E.; Mulder, R. J.; Rizzardo, E.; Gu, M.; Raston, C. L. *Chem. Mater.* **2010**, *22*, 4135–4143.
(72) Evans, C. M.; Evans, M. E.; Krauss, T. D. *J. Am. Chem. Soc.* **2010**, *132*, 10973–10975.
(73) Clark, M.; Kumar, S.; Owen, J. S.; Chan, E. M., manuscript in preparation.

allowed to continue at this temperature. Aliquoting was begun immediately following the injection.

c. Aliquoting Procedure. Kinetics experiments analyzed with $\{^1H\}^{31}P$ NMR spectroscopy were conducted by hand. Aliquots (~0.2 mL) were removed via syringe and added to septum-sealed vials filled with argon. The mass of the aliquot was determined and an equal mass of toluene-d_8 added to dissolve the aliquot. Next, 0.6 mL of this solution was transferred to an NMR tube and the remainder diluted to a known concentration and an absorbance less than 0.50 at 350 nm.

High-Throughput Reactions. a. Stock Solutions. Cd-ODPA solutions in TOPO were prepared on 180−360 g scale and transferred to a glovebox under vacuum. The stock solution was then melted by reheating to 120 °C and dispensed into the 40 mL reaction vials. Recrystallized TOPO and recrystallized ODPA were added to the reaction vials to achieve the desired concentrations of those species (Table S1, Supporting Information). The total mass of reagent in each reaction vial was 10 g prior to injection of **1**.

b. Synthesis and Characterization. A detailed discussion of high-throughput methods is presented in the Supporting Information, and they have been described elsewhere.[31] Briefly, automated reactions were performed on the Workstation for Automated Nanomaterials Discovery and Analysis at the Molecular Foundry. Following the automated injection of **1**, 60 μL aliquots were taken at known time intervals and diluted 25-fold with *m*-xylene. A 200 μL sample of each of these solutions was added to a well on a 96-well quartz microtiter plate (Hellma) for UV−visible absorption and fluorescence spectroscopy. Spectra were acquired in a BioTek Synergy4 multifunction plate reader running Gen5 software. The wavelength steps were 2 nm, and acquisition times were 15 and 60 s per absorption and fluorescence spectrum, respectively. For fluorescence spectra, wells were excited from the top using 380 nm excitation from a high-intensity xenon flash lamp. Data at each wavelength step were averaged over 24 flashes.

UV−Visible Data Analysis. A detailed discussion of the aliquoting procedure was presented in our previous paper.[31] Using this procedure, the concentration of crystalline CdSe was measured from the absorbance of reaction aliquots diluted with toluene or xylene. After adjusting the baseline to zero in the region from 740 to 750 nm and correcting for the dilution of the aliquots, we extracted [CdSe] from the absorbance at $\lambda = 350$ nm (A_{350}) using the size-independent extinction coefficient published by Bawendi.[49] The peak absorption wavelength (λ_{max}) of the CdSe $1S_{1/2e}1S_{3/2h}$ transition in the spectrum of each aliquot was identified using the FindPeak function in Igor Pro. The mean diameters (d_{avg}) of the CdSe NCs were estimated from λ_{max} using an empirical sizing equation described by Yu et al.[48] The concentration of NCs was then estimated from [CdSe] and the NC volume assuming a monodisperse population and a molar volume equal to that of bulk CdSe. Precursor conversion rates (Q_o) were determined from the change in [CdSe] versus reaction time using the method of initial rates. For each kinetic trace, a line was fit to the first approximately six non-zero points, and the slope was used as a measure of Q_o (Figure S3, Supporting Information). Final particle concentrations, n_f, were determined by averaging the particle concentrations calculated in each aliquot after the initial fluctuation. A discussion of the uncertainty in these methods is presented in the Supporting Information.

Supporting Information Available: Discussion of error analysis used in this study, TEM of CdSe particles prepared using our optimized conditions, example high-throught absorption data, example straight line fits used to determine Q_o from [CdSe] versus time, the final number of nanocrystals versus the initial rate (Q_o) of the precursor conversion in reactions with **1−3**, precursor conversion and CdSe appearance data from reactions using preformed Cd-ODPA and simultaneous injection of $CdMe_2$ and **1**, appearance of CdSe across four concentrations of added **1** (0.25, 0.5, 1.0, 2.0 equiv) and three concentrations of ODPA (1.67, 1.72, 1.80 equiv), diameter data across several ratios of ODPA:Cd and **1**, experimental data from our studies on the dissolution of CdSe in TOPO and ODPA, and a proposed equilibrium expression describing cadmium selenide dissolution and crystallization. This material is available free of charge via the Internet at http://pubs.acs.org.

JA106777J